https://doi.org/10.5194/egusphere-2026-6635
Preprint. Discussion started: 23 November 2026
© Author(s) 2026. CC BY 4.0 License.

Synoptic analysis of glacial boulder and bedrock cosmogenic ^{10}Be data

Arvid Hill and Jakob Heyman

Department of Earth Sciences, University of Gothenburg, Gothenburg, 40530, Sweden

Correspondence to: Arvid Hill (gushillar@student.gu.se) and Jakob Heyman (jakob.heyman@gu.se)

https://doi.org/10.5194/egusphere-2026-6635
Preprint. Discussion started: 23 November 2026
© Author(s) 2026. CC BY 4.0 License.



Abstract

Cosmogenic dating is a major chronological tool within geomorphology. While cosmogenic nuclide measurement accuracy increases, cosmogenic dating typically relies on assumptions about the exposure history that are evaluated based on analysis of multiple samples from single sites. Biased cosmogenic accumulation skewing ages to older or younger than the true deglaciation or landform age is in this context usually difficult to determine and interpret, as erosion rates and shielding processes differ depending on several factors. This study is a synoptic ^{10}Be comparison of a large global dataset consisting of sample sites with samples from boulders (n = 14972) and bedrock (n = 3128), testing for a global sample-type-dependent age bias. We tested the data in three steps: (i) internally between boulder and bedrock samples within each site consisting of both sample types (n of pairs compared = 1648); (ii) sample type based through global chi-square clustering rates and global skewness values; and (iii) externally, compared to existing Eurasian and North American deglaciation chronologies to determine potential biases within each sample type. Internally, the median bedrock age is ~3.5 % older than for boulder samples and since neither clustering rates nor skewness values differ substantially, we identify a biased age difference. Compared to deglaciation chronologies, this bias is also evident as bedrock samples predominantly show older ages than the reference data, while boulder samples concentrate more closely around reconstructed deglaciation ages. The difference between bedrock and deglaciation ages tends to increase with elevation, with an onset at about 800 m a.s.l. We attribute this difference most likely to cosmogenic nuclide inheritance in bedrock surfaces located within high-elevation areas with conditions for cold-based ice, where limited erosion results in increased inherited nuclides from earlier exposure.

1. Introduction

The field of cosmogenic dating has improved substantially in past decades, with improved production rate calibrations (Balco et al., 2008; Balco et al., 2009; Borchers et al., 2016; Martin et al., 2017; Balco, 2020), increased precision in analytical measurements (Balco, 2011), and new methods to use and analyse cosmogenic data (Schaefer et al., 2022). As improvements in measurement precision continue, they also identify discrepancies between exposure ages and independent chronologies that were previously obscured by larger uncertainties (Balco, 2011).

Cosmogenic surface exposure dating builds on the assumption that a sample has been fully exposed ever since the event to be dated, but completely shielded from cosmic rays prior to this dating event (Gosse and Phillips, 2001; Putkonen and Swanson, 2003; Heyman et al., 2011). If these assumptions are not fulfilled the exposure age can be either too young or too old depending on the exposure history.

If a sample is shielded from cosmic rays during some period after the event to be dated, fewer cosmogenic nuclides than expected are produced resulting in a too young exposure age (Gosse and Phillips, 2001; Applegate et al., 2008; Balco, 2011; Heyman et al., 2011; Balco, 2020). A commonly noted case with post-glacial shielding is moraine boulders buried under sediments and later exhumed at the moraine surface (Hallet and Putkonen, 1994; Applegate et al., 2008; Heyman et al., 2011, 2016; Tomkins et al., 2021). Also, continuous surface erosion decreases the level of cosmogenic nuclides as the eroded material earlier shielded the sampled surface.

If, in contrast, a sample has experienced some exposure to cosmic rays before, more cosmogenic nuclides are produced than expected, and the exposure age will be older than the actual age. A common case with pre-glacial

https://doi.org/10.5194/egusphere-2026-6635
Preprint. Discussion started: 23 November 2026
© Author(s) 2026. CC BY 4.0 License.

exposure is when a sample has been collected from a site where only minor glacial erosion has occurred, so that the sample collected was indeed exposed to cosmic rays and cosmogenic nuclides produced before the last ice cover period (Briner et al., 2003; Fabel et al., 2002; Stroeven et al., 2002). For very young glacial boulders, predepositional exposure during supraglacial transportation can yield cosmogenic nuclide concentrations significantly higher than expected (Balco, 2011).

These cases of potential mismatches are common obstacles for cosmogenic dating studies. A common approach for evaluating the quality of the exposure ages is to date multiple samples from single sites. If the samples yield the same, or sufficiently similar, ages this can be used as an argument for the samples having experienced an exposure history that coincides with the ideal case assumptions. In an ideal case, all samples can be used interchangeably regardless of sample type – since any groups of well-clustered samples are considered a robust indicator of the landform age (Balco, 2011). If a systematic age bias towards older or younger exposure ages is present, the resulting chronology may not reflect the true age (Balco, 2020). These biases are usually attributed to shielding and erosion processes (Patton et al., 2022).

Samples used for glacial cosmogenic dating are primarily collected from boulders (on moraines and loose in the landscape) and from bedrock surfaces (Balco, 2011; Heyman, 2026a). These sample types have different erosion and exposure histories. While bedrock samples are derived from their original position, boulders have experienced removal from bedrock, transportation, and potentially multiple erosional and depositional events (Linge et al., 2006; Hein et al., 2014; Leger et al., 2023, 2026). As the prerequisites for geological processes are contextual, a risk of over- or underestimating ages is a tangible problem within the field (Applegate et al., 2010).

We quantify and compare cosmogenic age data for samples collected from boulders and bedrock using ^{10}Be ages from a global glacial dataset (Heyman, 2026a) to highlight systematic biases in age. This is conducted internally (between boulder and bedrock samples of the same site), by determining rates of well-clustered and right- or left skewed group IDs in both sample types, and through a reference comparison (against two multiproxy deglaciation chronologies) to determine the relation between the two sample types.

2. **Methodology**

2.1 Data

We use ^{10}Be data from the expage glacial data compilation version 202610 (Heyman, 2026a). This global compilation contains published cosmogenic data from glacial and glacially related settings including all necessary data for recalculation of exposure ages, metadata on source of data and assumptions/modifications for incomplete or erroneous data. As ^{10}Be is by far the most commonly used cosmogenic nuclide, we focus on ^{10}Be data only and include all ^{10}Be measurements from boulder samples (n = 14972) and bedrock samples (n = 3128) within 5759 sample sites for the analysis. The compilation contains glacially related samples in general, meaning that there are boulder and bedrock samples from many different settings. Boulders from moraine ridges make up for more than half the dataset but boulder and bedrock samples scattered across the landscape are also common.

We use the expage zero erosion ^{10}Be exposure age calculated with the expage calculator version 202610 (Heyman, 2026b), and thus, we assume no subaerial erosion for all samples. This calculator is based on the

https://doi.org/10.5194/egusphere-2026-6635
Preprint. Discussion started: 23 November 2026
© Author(s) 2026. CC BY 4.0 License.

CRONUS calculator v. 2 (Balco et al., 2008), and uses the nuclide-specific LSD scaling (Lifton et al., 2014) with muon parameterisation based on CRONUScalc and available depth profile data (Marrero et al., 2016; Balco, 2017), the geomagnetic framework of Lifton (2016), and a global ^{10}Be production rate based on 28 calibration sites (Heyman, 2026c).

Each cosmogenic nuclide measurement in the expage compilation has a sample ID and a group ID, where identical sample IDs indicate repeat measurements from a single sample and identical group IDs indicate that samples are derived from the same site and are expected to have the same deglaciation age. The group ID classification is typically based on information in the original publications such as division between separate moraine ridges or multiple groups of samples located close together. The classification involves some subjectivity and varies across contrasting landscapes. For example, grouped samples from the northern Hemisphere paleo-ice sheets, which covered vast areas and experienced rapid deglaciation, can be spaced farther apart than samples in alpine settings, where shorter distances often represent larger relative change in glacial extent. However, the classification is done consistently with the aim to enable synoptic analysis across diverse landscapes and glacier types.

For all samples with repeat measurements (identical sample IDs), we calculate weighted mean exposure ages using the internal uncertainty (Balco et al., 2008). Further, to not punish high precision measurements in the cluster analysis, we use the greater of either the reported internal age uncertainty, or 2.9 % of the calculated exposure age based on the repeat measurement data for high concentration ^{10}Be samples reported in Jull et al. (2015).

To optimise the coding process, we used the large language model Claude Opus 5.5 (Anthropic, 2026) for generating the main framework for the code conducting the calculations. All code was subsequently reviewed and modified by the authors.

2.2 Internal comparison

We internally compare all groups containing both bedrock and boulder samples to determine the differences of cosmogenic ages for each sample type from the same landform or site. This is done by pairing all bedrock samples with all boulder samples within the same group ID. We identify a total number of 379 groups consisting of 1477 sample IDs (Fig. 1). The total number of pairs within each group ID having at least one boulder and one bedrock sample sums up to 1648 pairings. Within these pairs we calculate the percentage differences using the youngest sample as the denominator. Additionally, we weight all pairs with the number of pairs of each group as denominators (1/n) for comparison, as it shows whether groups with uneven sample type distribution disproportionately affect the results.

https://doi.org/10.5194/egusphere-2026-6635
Preprint. Discussion started: 23 November 2026
© Author(s) 2026. CC BY 4.0 License.

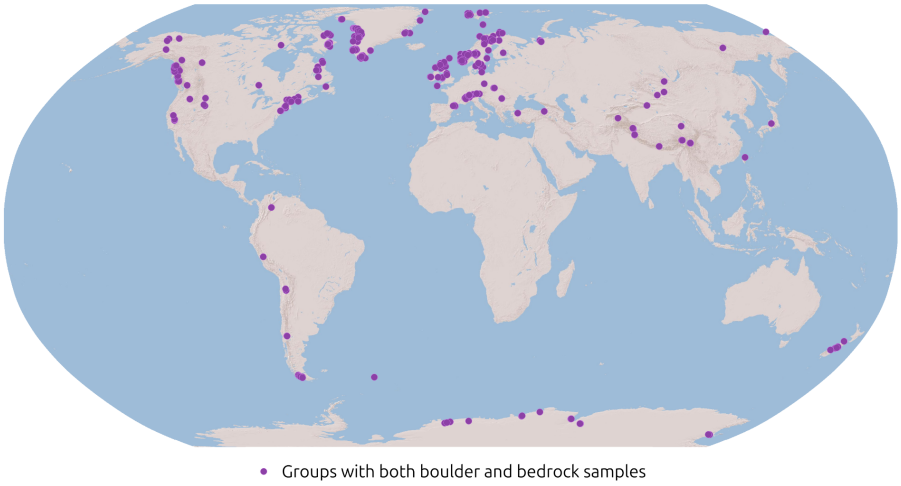

Figure 1: Global distribution of the 379 groups consisting of both boulder (n = 823) and bedrock (n = 654) samples, used for the internal comparisons.

2.3 Clustering and skewness analysis

We test how well each sample type clusters throughout all groups of the expage compilation, using all groups consisting of two or more samples respectively for each sample type. For this analysis we use a chi-square test for all groups with at least two samples of boulder or bedrock. The test assesses whether scatter exceeds measurement uncertainty, indicating incompatible exposure histories. To determine if a group of ages is clustered or scattered, we use a chi-square p-value threshold of 0.05 for the hypothesis that measurement uncertainty alone can explain the age scatter. For all scattered groups with three or more samples we exclude the sample with the largest deviation from the weighted mean age, taking uncertainties into account, allowing a maximum of one-third of the samples as outliers.

We also apply the same selection of data (sample type separately, group size-wise), but removing all groups of n = 2, to calculate skewness g_1 based on Applegate et al. (2010). Positive tails are explained by Applegate et al. (2010) as consistent with inheritance factors, and negative values with moraine degradation.

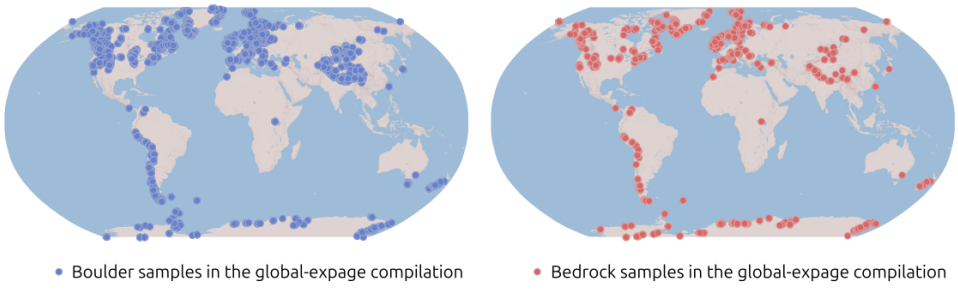

Figure 2: Global distribution of all boulder (n = 14972) and bedrock (n = 3128) samples in the compilation, from which the clustering (groups of ≥ 2 samples) and skewness (groups of ≥ 3 samples) subsets are drawn, used for the clustering and skewness analyses.

https://doi.org/10.5194/egusphere-2026-6635
Preprint. Discussion started: 23 November 2026
© Author(s) 2026. CC BY 4.0 License.

2.4 External validation

The expage compilation samples are also tested against the deglaciation chronology over the Eurasian and American ice sheets, interpolated from Hughes et al. (2016) and Dalton et al. (2023). The deglaciation chronologies are interpolated stepwise for each pair of adjacent isochrons from old to young, with Euclidean distance linear interpolation between the isochrons, resulting in a spatially continuous reconstruction of the youngest deglaciation. We subtract the deglaciation ages from the compilation ^{10}Be ages, with positive residuals representing exposure ages older than the reconstructed deglaciation ages. In this article we use the term residual consistently as ^{10}Be ages minus the corresponding deglaciation age.

The reference chronologies (Hughes et al., 2016; Dalton et al., 2023) are multi-proxy reconstructions that include ^{10}Be and radiocarbon samples. Further, the reconstructions are largely based on radiocarbon dates. In many cases we use the same samples used in Hughes et al. (2016) and Dalton et al. (2023) for our calculations; however we mainly analyse potential systematic differences in age between sample types. As this difference is the central finding in this paper, the overlap in samples is not considered a methodological obstacle.

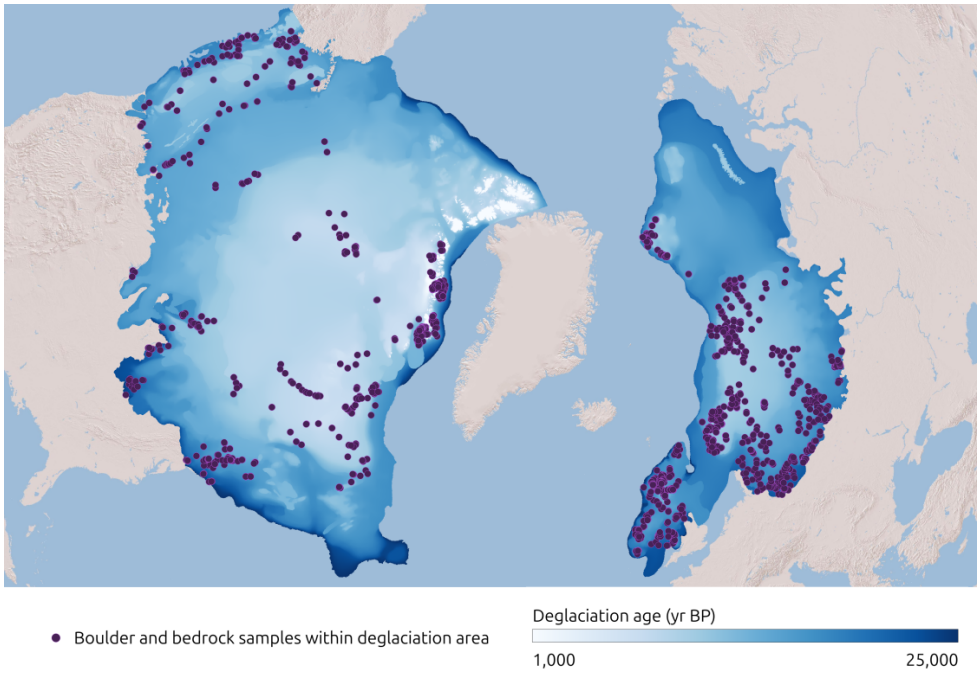

Figure 3: Distribution of all samples (n = 4282) used for comparison with the two ice sheet deglaciation chronologies from Hughes et al. (2016) for the European samples and Dalton et al. (2023) for the North American samples.

Samples taken in known previously submerged areas are corrected for nuclide accumulation suppressed during submergence. We use the relative sea level model of Påsse and Daniels (2015) for samples in Scandinavia (n = 97) and the ICE7G model (Peltier, 2020) for samples in Estonia and Lithuania (n = 13), and North America (n = 2). Groups consisting of samples collected to date late Holocene ages are removed as we do not expect them to correspond to deglaciation ages. As the reference ages are calculated from 1950, these ages are corrected

https://doi.org/10.5194/egusphere-2026-6635
Preprint. Discussion started: 23 November 2026
© Author(s) 2026. CC BY 4.0 License.

relative to the year of each sampling.

3. Results

3.1 Internal group based comparisons

Within the group based internal comparisons (Fig. 4) bedrock ages exceed boulder ages in 57 % of the comparisons and boulder ages exceed bedrock ages in 43 %. The median percentage difference is 3.54 %, and the median difference is 408 years, both indicating systematically older bedrock. The distribution of differences centres around this median, with a slightly right-skewed positive tail, indicating that large positive deviations (prominently older bedrock) are more common than large negative deviations (prominently older boulder). When weighting the pairs by 1/n, bedrock samples showed an age difference median of 5.33 %, indicating older bedrock ages. With this weighting 61.1 % of the summed weight showed older ages for bedrock samples, while 38.9 % had older boulder samples.

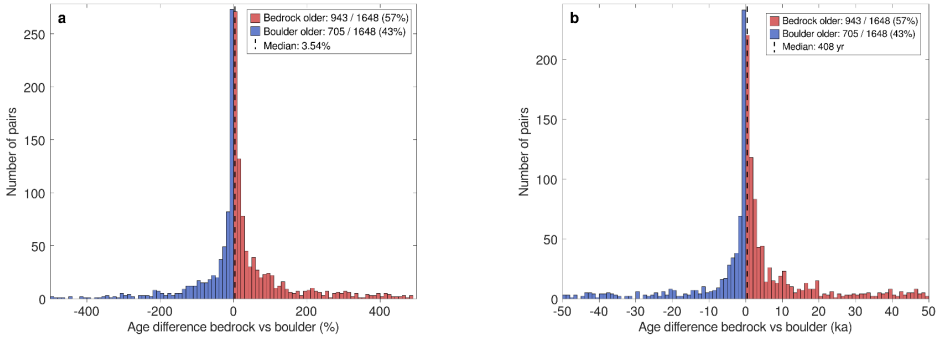

Figure 4: Histograms of paired differences in age, visualising the distribution of differences in relation to magnitude. The plot shows calculations both normalised (a, left) and absolute (b, right).

3.2 Cluster coherence and skewness by sample type

From the chi-square test boulder and bedrock samples show similar clustering rates (Fig. 5). Samples are well-clustered without outlier removal in 37.9 % of boulder groups, and 44.9 % of bedrock groups (Fig. 5). When removing outliers, clustering rates for boulder samples are 59.2 %, and for bedrock 58.0 % (Fig. 5). The clustering rates with outlier removal are greater within the boulder data, making the total clustering rates similar given our threshold criteria.

https://doi.org/10.5194/egusphere-2026-6635
Preprint. Discussion started: 23 November 2026
© Author(s) 2026. CC BY 4.0 License.

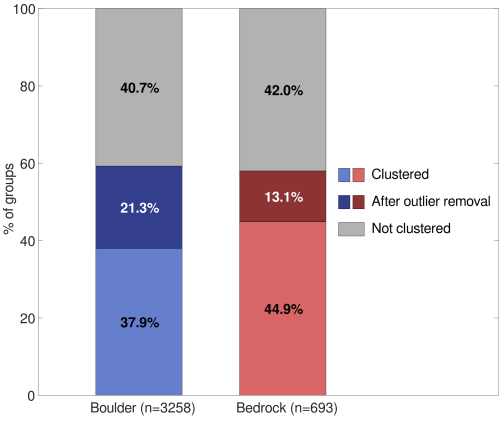

175

176 **Figure 5:** Proportion of well-clustered groups with and without the removal of outliers for the entire dataset for
177 each sample type.

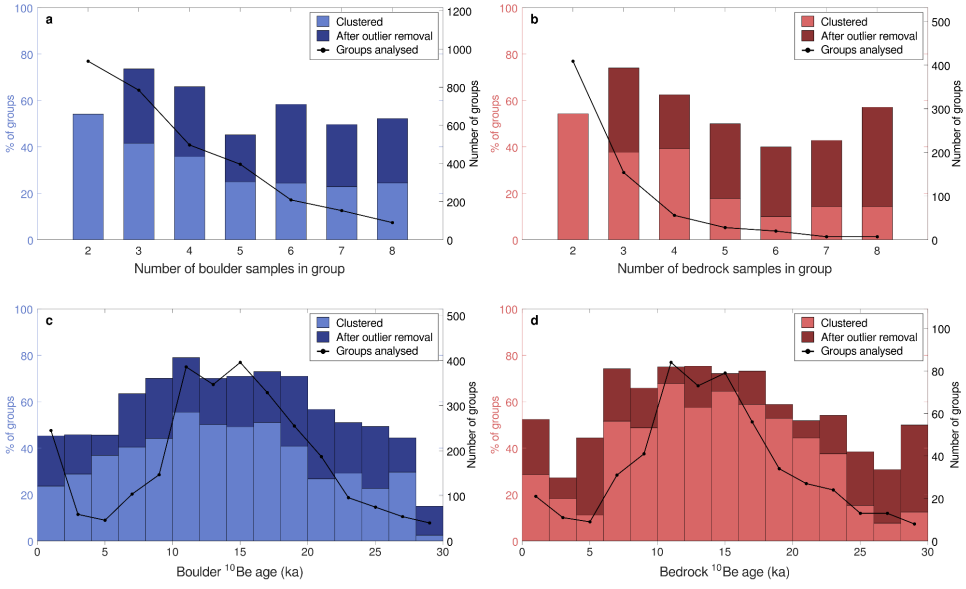

178

179 **Figure 6:** Clustering rates for each sample type in relation to the number of samples per group (a, b) and to ^{10}Be
180 ages (c, d). Coloured parts are read against the left y-axis and the black line represents the number of groups
181 read on the right y-axis. As groups with only one boulder or bedrock sample cannot be tested for clustering,
182 those are not represented in the figure, and groups of >8 samples are excluded as they are too few.

183 Clustering rates decrease with group size (Fig. 6a, b). Groups consisting of two to four samples dominate the
184 data (groups of two samples are particularly dominant within the bedrock distribution) and have similar
185 clustering rates between the sample types. Boulder groups with five or more samples cluster slightly better than
186 bedrock groups, but there are relatively few bedrock groups within this range. Well-clustered groups peak
187 around 10–18 ka for both sample types (Fig. 6c, d), and the clustering rates coincide with the increased sample

https://doi.org/10.5194/egusphere-2026-6635
Preprint. Discussion started: 23 November 2026
© Author(s) 2026. CC BY 4.0 License.

density for both sample types in this age range.

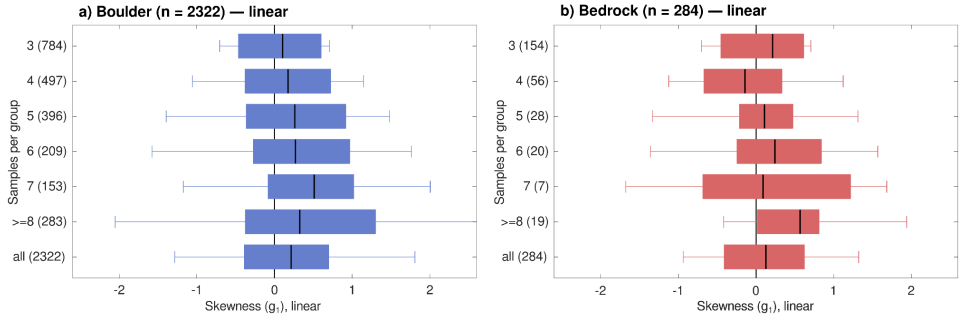

Figure 7: Groupwise skewness values of each sample type separately. Boxes represent the IQR of each calculation and whiskers 2.5th–97.5th percentiles. The black line represents the median of each distribution. Only groups of ≥ 3 samples are used for this analysis. Each bottom row shows the pooled distribution of all groups for a simplified summary of each sample type.

For both boulder and bedrock samples, more groups have positive than negative skewness, and at a synoptic scale they have generally similar skewness data (Fig. 7). The pooled value at the bottom of each graph does not show any visible systematic difference between sample types, with a median g_1 value of 0.214 for boulder and 0.126 for bedrock.

3.3 Comparisons to reference dataset

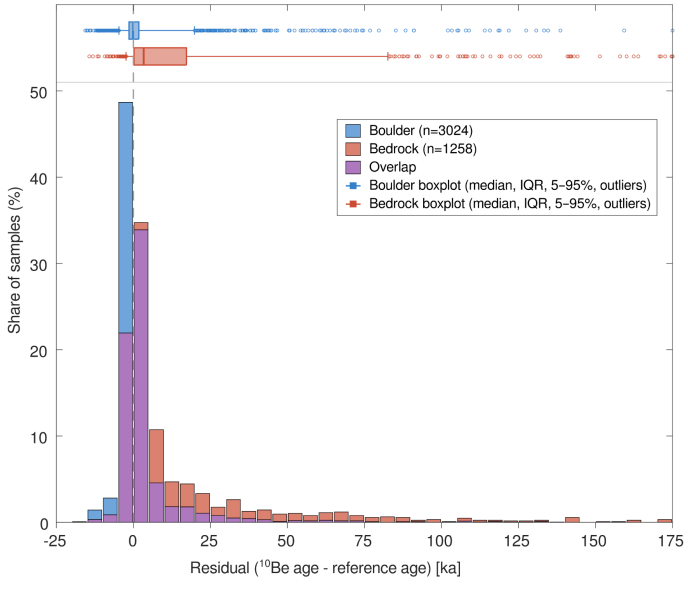

Figure 8: Plots summarising age residuals. Boxplots show interquartile range (IQR) with whiskers extending to the 5th and 95th percentiles, with points beyond these limits shown as outliers. The histogram shows the

https://doi.org/10.5194/egusphere-2026-6635
Preprint. Discussion started: 23 November 2026
© Author(s) 2026. CC BY 4.0 License.

normalised distribution of age residuals for boulder and bedrock samples. The differences in distribution, where the two sample types dominate different residual intervals, are illustrated by surpluses above the purple columns.

Comparing the global compilation ^{10}Be data to the reference deglaciation ages, the boulder data has a median residual value of -128 years (-1.0 % younger than reference), compared to the bedrock median of 3354 years (26 % older than reference). Of 3024 boulder samples, 1602 (53 %) samples show younger ages than their reference counterparts and 1420 (47 %) older, while of 1258 bedrock samples 291 (23 %) show younger ages and 967 (77 %) older. The scatter of the residuals differs substantially between the sample types (Figs. 8; 9), with interquartile range (mid 50 %) of each sample type with values of -1.4 ka to +1.8 ka for boulder and +0.2 ka to +17.2 ka for bedrock. Boulder samples are more closely concentrated around reconstructed deglaciation ages, with a narrower interquartile range around zero. Bedrock samples show a larger portion of positive residuals and a wider interquartile range representing greater residual variability.

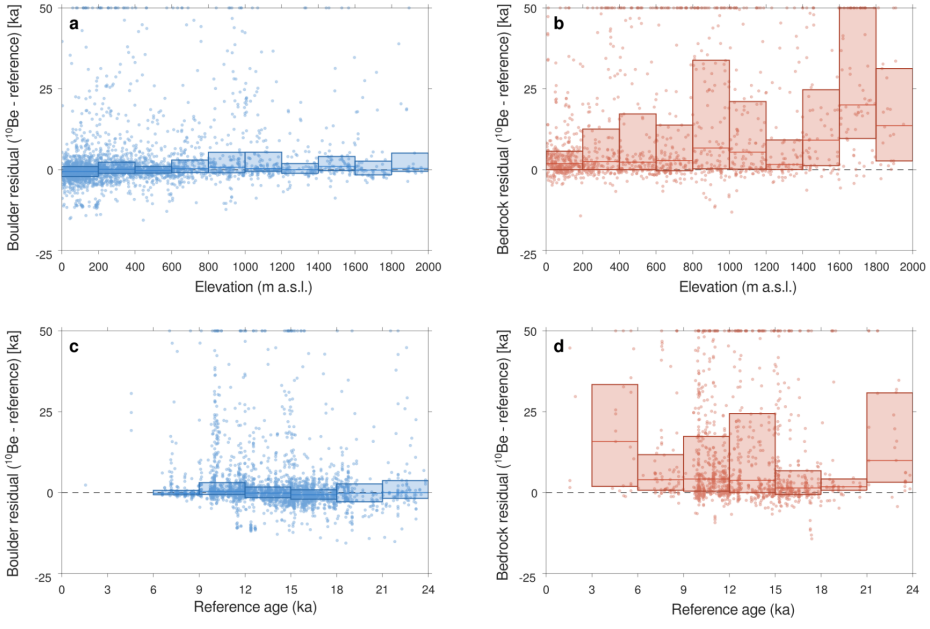

Figure 9: Panels (a) and (b) show boxplot (IQR) graphs consisting of residuals in relation to elevation for boulder and bedrock data. Panels (c) and (d) show boxplot (IQR) graphs consisting of residuals in relation to reference ages of the Hughes et al. (2016) and Dalton et al. (2023) rasters.

Compared against elevation (Fig. 9), bedrock residuals are visibly greater than the reference data. Starting with a median residual at <5 ka at low elevations, a rise in residuals takes place at ~800 m a.s.l. with further increase at higher elevations. Boulder residuals differ systematically from bedrock residuals, with the median value being consistently close to reference age even at higher elevations.

Compared against reference ages, bedrock samples show a larger scatter than boulder samples, with older median ages throughout the dataset. The interquartile range (Q1–Q3 boxes) illustrates this distribution difference, though there are no deglaciation age-dependent trends (Fig. 9c, d) but rather a general difference

https://doi.org/10.5194/egusphere-2026-6635
Preprint. Discussion started: 23 November 2026
© Author(s) 2026. CC BY 4.0 License.

throughout the full range.

4. Discussion

Globally, bedrock samples are systematically older than their boulder counterparts, with a median age difference of ~3.5 % or 408 years (Fig. 4), but this difference is obscured by large internal variation and close to 40 % of the comparisons have boulder samples older than bedrock samples. Whether true deglaciation ages are best reflected by boulder or bedrock samples cannot be determined from the internal comparisons alone. The systematic age difference between boulder and bedrock samples is not reflected in the clustering analysis, and skewness values do not differ enough to distinguish the sample types from each other (Fig. 7). The difference is, however, evident in the comparison with deglaciation chronologies (Fig. 8).

The total clustering values (Fig. 5) are affected by the distribution of group sizes (Fig. 6) within the two sample types, as groups with fewer samples cluster more easily. Well-clustered groups concentrate, for both sample types, around 10–18 ka (Fig. 6), matching the time period of global deglaciation (Shakun et al., 2015; Hughes et al., 2016; Dalton et al., 2023). This clustering relation (deglaciation period is reflected by well-clustered samples) is consistent with previous studies (Heyman et al., 2016; Jandová, 2025).

In relation to the deglaciation chronologies of the European and American ice sheets, bedrock typically exceeds reference ages (median of +3354 years) while boulders track deglaciation more closely (median of -128 years), identifying cosmogenic nuclide inheritance as a likely stronger factor for bedrock samples than shielding processes for boulder samples.

The boulder sample residuals are evenly distributed older or younger than the reference age (Fig. 8). The tight interquartile range indicates that samples in half the cases represent deglaciation ages reasonably well, but the outliers show that still a large portion of samples deviate in a broad range of younger or older ages. In contrast to boulder interquartile range distribution, bedrock samples are more scattered and show systematically older ages than boulder samples. The residuals have a systematic increase with elevation, as high-elevation samples reveal larger offsets. The increase becomes particularly pronounced around 800 m a.s.l. and continues with elevation – a pattern previously identified in several studies (e.g. Goehring et al., 2008; Fabel et al., 2012; Briner et al., 2014; Andersen et al., 2020).

Erosion rates differ depending on whether a glacier is cold- or warm-based as basal meltwater enables sliding and abrasion (Sugden, 1968; Kleman, 1994; Goehring et al., 2008; Patton et al., 2022). The likelihood of cold-based ice increases with elevation (Briner et al., 2006; Goehring et al., 2008) – which harmonises with our findings (Fig. 9a, b), as insufficient erosion is a likely cause of increased inheritance of cosmogenic nuclides (Bierman et al., 1999; Stroeven et al., 2002; Briner et al., 2003).

Cosmogenic inheritance due to insufficient erosion is generally attributed to temperature variations depending on ice thickness, as thicker ice generates more basal meltwater and glacial ice thins with elevation (Sugden et al., 2005). Unlike boulder samples, bedrock samples are not quarried and transported before sampling (Alley et al., 2019), which makes them dependent on erosion in situ. As cold-based conditions are likely to reduce glacial erosion, bedrock surfaces will retain inherited nuclide concentrations from prior exposure.

Given that boulder ages better align with deglaciation chronologies compared to bedrock ages, which typically exceed them (Fig. 8), insufficient bedrock erosion is a likely primary cause for the internal discrepancy and the

https://doi.org/10.5194/egusphere-2026-6635
Preprint. Discussion started: 23 November 2026
© Author(s) 2026. CC BY 4.0 License.

deglaciation residual comparison. However, the underlying dynamics are complex, as earlier studies have shown it likely that boulder samples within moraines are more susceptible to shielding processes (Applegate et al., 2008, 2010; Heyman et al., 2011; Zreda and Phillips, 1995). The analysis highlights age differences but both prior and incomplete exposure can simultaneously affect the data at a synoptic scale, making it difficult to isolate the individual processes leading to older or younger ages.

If higher ages of bedrock compared to boulder samples can be explained by more cosmogenic nuclide inheritance in bedrock, we would expect that groups of bedrock samples yield more positive skewness compared to boulder samples (Applegate et al., 2010), but this is not visible in the synoptic scale data (Fig. 7). The lack of skewness difference between boulder and bedrock samples potentially hints either that cosmogenic nuclide inheritance dominates for both bedrock and boulder samples, or, more likely, that the signature of cosmogenic nuclide inheritance overprints the effect of incomplete exposure yielding negative skewness.

A subset of the global dataset (Heyman, 2026a) consists of studies specifically designed to test for limited erosion resulting in increased cosmogenic nuclide inheritance (e.g. Stroeven et al., 2002; Fabel et al., 2002; Briner et al., 2003; Phillips et al. 2006). Such studies have primarily targeted bedrock samples, sampling bedrock expected to yield older ages than those indicated by existing deglaciation chronologies, frequently in high-elevation areas where cold-based conditions are likely. This subset may therefore enhance the elevation-dependent trend in bedrock residuals (Fig. 9b). The overall conclusions are unlikely to be altered by this subset, since bedrock residuals exceed boulder residuals across the full elevation range (also below 800 m a.s.l.) and regardless of deglaciation age (Fig. 9c, d).

5. Conclusions

Comparing the two sample types, bedrock samples show a higher age both internally for the global dataset and in relation to the Northern Hemisphere ice sheet deglaciation chronologies. The age difference is systematic but context-dependent. The following conclusions have been identified:

i) bedrock samples systematically yield older ages than boulder samples; however these differences are not exceptionally large (a relation of ~60 %/40 %) and the age difference between the sample types varies widely within different groups.

ii) bedrock and boulder sample types show no discernible difference in clustering rates or skewness values and neither sample type performs markedly better than the other, indicating similar scatter profiles within both sample types.

iii) for the Northern Hemisphere paleo-ice sheets, boulder samples yield ages closer to the deglaciation chronology compared to their bedrock counterparts. Bedrock samples yield older ages likely due to cosmogenic nuclide inheritance and the age difference increases with elevation.

Code and data availability

Data and code are available at https://doi.org/10.5281/zenodo.23335584 (Hill and Heyman, 2026). Open the README file for information on the contents.

Author contributions

https://doi.org/10.5194/egusphere-2026-6635
Preprint. Discussion started: 23 November 2026
© Author(s) 2026. CC BY 4.0 License.

AH and JH conceptualised the study and compiled cosmogenic nuclide data. AH developed models for calculations. AH and JH conducted the analysis. AH prepared the manuscript with contributions from JH.

Competing interests

The authors declare that they have no conflict of interest.

References

Alley, R. B., Cuffey, K. M., and Zoet, L. K.: Glacial erosion: status and outlook, Ann. Glaciol., 60, 1–13, https://doi.org/10.1017/aog.2019.38, 2019.

Andersen, J. L., Egholm, D. L., Olsen, J., Larsen, N. K., and Knudsen, M. F.: Topographical evolution and glaciation history of South Greenland constrained by paired 26Al/10Be nuclides, Earth Planet. Sci. Lett., 542, 116300, https://doi.org/10.1016/j.epsl.2020.116300, 2020.

Anthropic: Claude Opus 5.5 [large language model], https://platform.claude.com/docs/en/models/opus-5-5/overview (last access: 30 September 2026), 2026.

Applegate, P. J., Lowell, T. V., and Alley, R. B.: Comment on "Absence of Cooling in New Zealand and the Adjacent Ocean During the Younger Dryas Chronozone", Science, 320, 746–746, https://doi.org/10.1126/science.1152098, 2008.

Applegate, P. J., Urban, N. M., Laabs, B. J. C., Keller, K., and Alley, R. B.: Modeling the statistical distributions of cosmogenic exposure dates from moraines, Geosci. Model Dev. 3, 293–307, https://doi.org/10.5194/gmd-3-293-2010, 2010.

Balco, G.: Contributions and unrealized potential contributions of cosmogenic-nuclide exposure dating to glacier chronology, 1990–2010, Quat. Sci. Rev., 30, 3–27, https://doi.org/10.1016/j.quascirev.2010.11.003, 2011.

Balco, G.: Production rate calculations for cosmic-ray-muon-produced 10Be and 26Al benchmarked against geological calibration data, Quat. Geochronol., 39, 150–173, https://doi.org/10.1016/j.quageo.2017.02.001, 2017.

Balco, G.: Glacier Change and Paleoclimate Applications of Cosmogenic-Nuclide Exposure Dating, Annu. Rev. Earth Planet. Sci., 48, 21–48, https://doi.org/10.1146/annurev-earth-081619-052609, 2020.

Balco, G., Stone, J. O., Lifton, N. A., and Dunai, T. J.: A complete and easily accessible means of calculating surface exposure ages or erosion rates from 10Be and 26Al measurements, Quat. Geochronol., 3, 174–195, https://doi.org/10.1016/j.quageo.2007.12.001, 2008.

Balco, G., Briner, J., Finkel, R. C., Rayburn, J. A., Ridge, J. C., and Schaefer, J. M.: Regional beryllium-10 production rate calibration for late-glacial northeastern North America, Quat. Geochronol., 4, 93–107, https://doi.org/10.1016/j.quageo.2008.09.001, 2009.

Bierman, P. R., Marsella, K. A., Patterson, C., Davis, P. T., and Caffee, M.: Mid-Pleistocene cosmogenic minimum-age limits for pre-Wisconsinan glacial surfaces in southwestern Minnesota and southern Baffin Island: a multiple nuclide approach, Geomorphology, 27, 25–39,

https://doi.org/10.5194/egusphere-2026-6635
Preprint. Discussion started: 23 November 2026
© Author(s) 2026. CC BY 4.0 License.

https://doi.org/10.1016/S0169-555X(98)00088-9, 1999.

Borchers, B., Marrero, S., Balco, G., Caffee, M., Goehring, B., Lifton, N., Nishiizumi, K., Phillips, F., Schaefer, J., and Stone, J.: Geological calibration of spallation production rates in the CRONUS-Earth project, Quat. Geochronol., 31, 188–198, https://doi.org/10.1016/j.quageo.2015.01.009, 2016.

Briner, J. P., Miller, G. H., Davis, P. T., Bierman, P. R., and Caffee, M.: Last Glacial Maximum ice sheet dynamics in Arctic Canada inferred from young erratics perched on ancient tors, Quat. Sci. Rev., 22, 437–444, https://doi.org/10.1016/S0277-3791(03)00003-9, 2003.

Briner, J.P., Miller, G. H., Davis, P. T., and Finkel, R. C.: Cosmogenic radionuclides from fiord landscapes support differential erosion by overriding ice sheets, GSA Bull., 118, 406–420, https://doi.org/10.1130/B25716.1, 2006.

Briner, J. P., Lifton, N. A., Miller, G. H., Refsnider, K., Anderson, R., and Finkel, R. C.: Using in situ cosmogenic 10Be, 14C, and 26Al to decipher the history of polythermal ice sheets on Baffin Island, Arctic Canada, Quat. Geochronol., 19, 4–13, https://doi.org/10.1016/j.quageo.2012.11.005, 2014.

Corbett, L. B., Young, N. E., Bierman, P. R., Briner, J. P., Neumann, T. A., Rood, D. H., and Graly, J. A.: Paired bedrock and boulder 10Be concentrations resulting from early Holocene ice retreat near Jakobshavn Isfjord, western Greenland, Quat. Sci. Rev., 30, 1739–1749, https://doi.org/10.1016/j.quascirev.2011.04.001, 2011.

Dalton, A. S., Dulfer, H. E., Margold, M., Heyman, J., Clague, J. J., Froese, D. G., Gauthier, M. S., Hughes, A. L. C., Jennings, C. E., Norris, S. L., and Stoker, B. J.: Deglaciation of the North American ice sheet complex in calendar years based on a comprehensive database of chronological data: NADI-1, Quat. Sci. Rev., 321, 108345, https://doi.org/10.1016/j.quascirev.2023.108345, 2023.

Fabel, D., Stroeven, A. P., Harbor, J., Kleman, J., Elmore, D., and Fink, D.: Landscape preservation under Fennoscandian ice sheets determined from in situ produced 10Be and 26Al, Earth Planet. Sci. Lett., 201, 397–406, https://doi.org/10.1016/S0012-821X(02)00714-8, 2002.

Fabel, D., Ballantyne, C. K., and Xu, S.: Trimlines, blockfields, mountain-top erratics and the vertical dimensions of the last British–Irish Ice Sheet in NW Scotland, Quat. Sci. Rev., 55, 91–102, https://doi.org/10.1016/j.quascirev.2012.09.002, 2012.

Goehring, B. M., Brook, E. J., Linge, H., Raisbeck, G. M., and Yiou, F.: Beryllium-10 exposure ages of erratic boulders in southern Norway and implications for the history of the Fennoscandian Ice Sheet, Quat. Sci. Rev., 27, 320–336, https://doi.org/10.1016/j.quascirev.2007.11.004, 2008.

Gosse, J. C. and Phillips, F. M.: Terrestrial in situ cosmogenic nuclides: theory and application, Quat. Sci. Rev., 20, 1475–1560, https://doi.org/10.1016/S0277-3791(00)00171-2, 2001.

Gosse, J. C., Klein, J., Evenson, E. B., Lawn, B., and Middleton, R.: Beryllium-10 Dating of the Duration and Retreat of the Last Pinedale Glacial Sequence, Science, 268, 1329–1333, https://doi.org/10.1126/science.268.5215.1329, 1995.

Hallet, B. and Putkonen, J.: Surface Dating of Dynamic Landforms: Young Boulders on Aging Moraines, Science, 265, 937–940, https://doi.org/10.1126/science.265.5174.937, 1994.

https://doi.org/10.5194/egusphere-2026-6635
Preprint. Discussion started: 23 November 2026
© Author(s) 2026. CC BY 4.0 License.

Hein, A. S., Fogwill, C. J., Sugden, D. E., and Xu, S.: Geological scatter of cosmogenic-nuclide exposure ages in the Shackleton Range, Antarctica: Implications for glacial history, Quat. Geochronol., 19, 52–66, https://doi.org/10.1016/j.quageo.2013.03.008, 2014.

Heyman, J.: expage version 202610, Zenodo [data set], https://doi.org/10.5281/zenodo.23351633, 2026a.

Heyman, J.: expage-calculator version 202610, Zenodo [code], https://doi.org/10.5281/zenodo.23351693, 2026b.

Heyman, J.: expage-production version 202610, Zenodo [data set], https://doi.org/10.5281/zenodo.23351678, 2026c.

Heyman, J., Stroeven, A. P., Harbor, J. M., and Caffee, M. W.: Too young or too old: Evaluating cosmogenic exposure dating based on an analysis of compiled boulder exposure ages, Earth Planet. Sci. Lett., 302, 71–80, https://doi.org/10.1016/j.epsl.2010.11.040, 2011.

Heyman, J., Applegate, P. J., Blomdin, R., Gribenski, N., Harbor, J. M., and Stroeven, A. P.: Boulder height – exposure age relationships from a global glacial Be-10 compilation, Quat. Geochronol., 34, 1–11, https://doi.org/10.1016/j.quageo.2016.03.002, 2016.

Hill, A. and Heyman, J.: Scripts and data for a synoptic analysis of glacial boulder and bedrock cosmogenic 10Be data (v1.0), Zenodo [code], https://doi.org/10.5281/zenodo.23335584, 2026.

Hughes, A. L. C., Gyllencreutz, R., Lohne, Ø. S., Mangerud, J., and Svendsen, J. I.: The last Eurasian ice sheets – a chronological database and time-slice reconstruction, DATED-1, Boreas, 45, 1–45, https://doi.org/10.1111/bor.12142, 2016.

Jandová, A.: Dating of moraines by cosmogenic isotopes, M.S. thesis, Charles University, Prague, Czech Republic, 91 pp., https://hdl.handle.net/20.500.11956/201783 (last access 28 October 2026), 2025.

Jull, A. J. T., Scott, E. M., and Bierman, P.: The CRONUS-Earth inter-comparison for cosmogenic isotope analysis, Quat. Geochronol., 26, 3–10, https://doi.org/10.1016/j.quageo.2013.09.003, 2015.

Kleman, J.: Preservation of landforms under ice sheets and ice caps, Geomorphology, 9, 19–32, https://doi.org/10.1016/0169-555X(94)90028-0, 1994.

Leger, T. P. M., Hein, A. S., Rodés, Á., Bingham, R. G., Schimmelpfennig, I., Fabel, D., and Tapia, P.: A cosmogenic nuclide-derived chronology of pre-Last Glacial Cycle glaciations during MIS 8 and MIS 6 in northern Patagonia, Clim. Past., 19, 35–59, https://doi.org/10.5194/cp-19-35-2023, 2023.

Leger, T. P. M., Jouvet, G., Kamleitner, S., Finley, B. D., Bernard, M., Allegri, B., Herman, F., Vieli, A., Henz, A., & Nussbaumer, S. U.: First Alps-wide reconstruction of LGM glacial sediment transport enabled by GPU-accelerated particle tracking, Earth Surf. Dyn., 14, 361–389, https://doi.org/10.5194/esurf-14-361-2026, (2026).

Lifton, N.: Implications of two Holocene time-dependent geomagnetic models for cosmogenic nuclide production rate scaling, Earth Planet. Sci. Lett., 433, 257–268, https://doi.org/10.1016/j.epsl.2015.11.006, 2016.

Lifton, N., Sato, T., and Dunai, T. J.: Scaling in situ cosmogenic nuclide production rates using analytical

https://doi.org/10.5194/egusphere-2026-6635
Preprint. Discussion started: 23 November 2026
© Author(s) 2026. CC BY 4.0 License.

approximations to atmospheric cosmic-ray fluxes, Earth Planet. Sci. Lett., 386, 149–160, https://doi.org/10.1016/j.epsl.2013.10.052, 2014.

Linge, H., Larsen, E., Kjær, K. H., Demidov, I. N., Brook, E. J., Raisbeck, G. M., and Yiou, F.: Cosmogenic 10Be exposure age dating across Early to Late Weichselian ice-marginal zones in northwestern Russia, Boreas, 35, 576–586, https://doi.org/10.1080/03009480600781909, 2006.

Marrero, S. M., Phillips, F. M., Borchers, B., Lifton, N., Aumer, R., and Balco, G.: Cosmogenic nuclide systematics and the CRONUScalc program, Quat. Geochronol., 31, 160–187, https://doi.org/10.1016/j.quageo.2015.09.005, 2016.

Martin, L. C. P., Blard, P.-H., Balco, G., Lavé, J., Delunel, R., Lifton, N., and Laurent, V.: The CREp program and the ICE-D production rate calibration database: A fully parameterizable and updated online tool to compute cosmic-ray exposure ages, Quat. Geochronol., 38, 25–49, https://doi.org/10.1016/j.quageo.2016.11.006, 2017.

Påsse, T. and Daniels, J.: Past shore-level and sea-level displacements, Rapporter och meddelanden 137, Sveriges geologiska undersökning, Uppsala, Sweden, 33 pp., https://resource.sgu.se/dokument/publikation/rm/rm137rapport/rm137-rapport.pdf (last access 28 October 2026), 2015.

Patton, H., Hubbard, A., Heyman, J., Alexandropoulou, N., Winsborrow, M., Lasabuda, A. P. E., Kleman, J., Andreassen, K. M., Sugden, D. E., Stroeven, A. P., and Hall, A. M.: The extreme yet transient nature of glacial erosion, Nat. Commun., 13, 7377, https://doi.org/10.1038/s41467-022-35072-0, 2022.

Peltier, W. R.: The ICE-7G_NA (VM7) Ice thickness and paleotopography 0–26 ka, Borealis [data set], V1, https://doi.org/10.5683/SP2/ZCDLY1, 2020.

Phillips, W. M., Hall, A. M., Mottram, R., Fifield, L. K., and Sugden, D. E.: Cosmogenic 10Be and 26Al exposure ages of tors and erratics, Cairngorm Mountains, Scotland: Timescales for the development of a classic landscape of selective linear glacial erosion, Geomorphology, 73, 222–245, https://doi.org/10.1016/j.geomorph.2005.06.009, 2006.

Putkonen, J., and Swanson, T.: Accuracy of cosmogenic ages for moraines, Quat. Res., 59, 255–260, https://doi.org/10.1016/S0033-5894(03)00006-1, 2003.

Schaefer, J. M., Codilean, A. T., Willenbring, J. K., Lu, Z.-T., Keisling, B., Fülöp, R.-H., and Val, P.: Cosmogenic nuclide techniques, Nature Reviews Methods Primers, 2, 18, https://doi.org/10.1038/s43586-022-00096-9, 2022.

Shakun, J. D., Clark, P. U., He, F., Lifton, N. A., Liu, Z., and Otto-Bliesner, B. L.: Regional and global forcing of glacier retreat during the last deglaciation, Nat. Commun., 6, 8059, https://doi.org/10.1038/ncomms9059, 2015.

Stroeven, A. P., Fabel, D., Hättestrand, C., and Harbor, J.: A relict landscape in the centre of Fennoscandian glaciation: cosmogenic radionuclide evidence of tors preserved through multiple glacial cycles, Geomorphology, 44, 145–154, https://doi.org/10.1016/S0169-555X(01)00150-7, 2002.

Sugden, D. E.: The selectivity of glacial erosion in the Cairngorm Mountains, Scotland, Trans. Inst. Br. Geogr.,

https://doi.org/10.5194/egusphere-2026-6635
Preprint. Discussion started: 23 November 2026
© Author(s) 2026. CC BY 4.0 License.



441 45, 79–92, https://doi.org/10.2307/621394, 1968.

442 Sugden, D. E., Balco, G., Cowdery, S. G., Stone, J. O., and Sass, L. C.: Selective glacial erosion and weathering
443 zones in the coastal mountains of Marie Byrd Land, Antarctica, Geomorphology, 67, 317–334,
444 https://doi.org/10.1016/j.geomorph.2004.10.007, 2005.

445 Tomkins, M. D., Dortch, J. M., Hughes, P. D., Huck, J. J., Pallàs, R., Rodés, Á., Allard, J. L., Stimson, A. G.,
446 Bourlès, D., Rinterknecht, V., Jomelli, V., Rodríguez-Rodríguez, L., Copons, R., Barr, I. D., Darvill, C. M., and
447 Bishop, T.: Moraine crest or slope: An analysis of the effects of boulder position on cosmogenic exposure age,
448 Earth Planet. Sci. Lett., 570, 117092, https://doi.org/10.1016/j.epsl.2021.117092, 2021.

449 Zreda, M. G., and Phillips, F. M.: Insights into alpine moraine development from cosmogenic 36Cl buildup
450 dating, Geomorphology, 14, 149–156, https://doi.org/10.1016/0169-555X(95)00055-9, 1995.